Supplementary information

High-sensitivity lanthanide ratiometric nanothermometer in the second biological window through bidirectional thermal response engineering

Shuohan Sun, [a] Dekang Huang, [a] Dan Li, [b] Mochen Jia [c] and Guanying Chen *[b]

[a]*School of Chemistry, Huazhong Agricultural University, Wuhan 430070, China.*

[b]*MIIT Key Laboratory of Critical Materials Technology for New Energy Conversion and Storage, School of Chemistry and Chemical Engineering & Key Laboratory of Micro-systems and Micro-structures, Ministry of Education, Harbin Institute of Technology, Harbin 150001, China.*

[c]Key Laboratory of Materials Physics of Ministry of Education, School of Physics, Zhengzhou University, Zhengzhou 450052, China.

Characterizations. The size and morphology of the nanoparticles were measured by the transmission electron microscope (TEM, JEM 1200EX). The Powder X-ray diffraction (XRD) patterns were detected by a BPUKER/D2PHASER diffractometer. Dynamic light scattering (DLS) were recorded on a Nano Zetasizer system (Malvern Instruments Ltd, UK). The luminescence spectra and decay curves were collected by Edinburgh FLS 1000 spectrofluorometer equipped with an 808 nm diode laser (MLL-III-808-2W, Changchun New Industries Optoelectronics Tech Co.) that could operate in both continuous-wave and pulse modes. The temperature-dependent spectra and decay curves were performed by a temperature-controlled cuvette holder equipped to the Edinburgh FLS1000 spectrofluorometer. The NIR quantum yield was determined using an integrating sphere in a steady-transisent fluorometer (Edingburg, FLS 1000). FT-IR spectra were recorded by a PerkinElmer 580B infrared spectrophotometer. NIR-II imaging was performedon a customized animal imaging system installed with an InGaAs camera (C-RED 2,France) and external laser diode emitting at 808 nm. The superficial thermography was recorded by an infrared thermal camera (Fotric 280s, Shanghai, China).

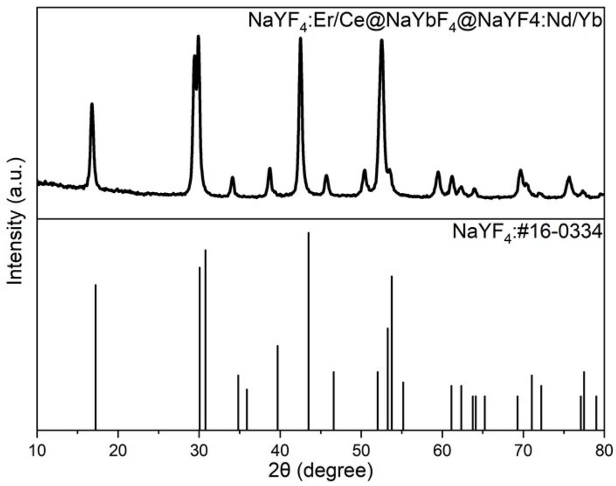

Fig. S1. X-ray diffraction pattern of the $NaYF_4:Er^{3+}/Ce^{3+}$@$NaYbF_4$@$NaYF_4:Nd^{3+}/Yb^{3+}$ nanoparticles and PDF card no.16-0334.

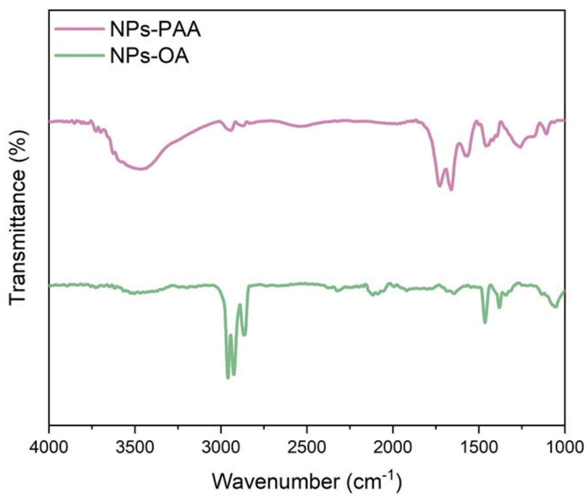

Fig. S2. FT-IR spectra of OA-capped and PAA-capped NPs.

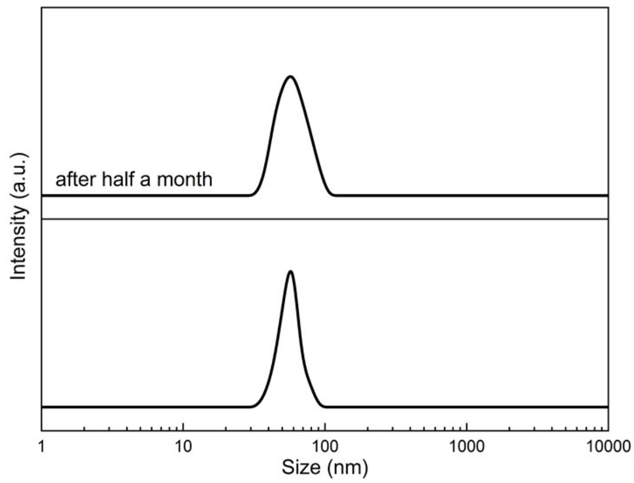

Fig. S3. Dynamic light scattering (DLS) size distribution of NPs (a) dissolved in phosphate-buffered saline (PBS) and (b) after storage for half a month.

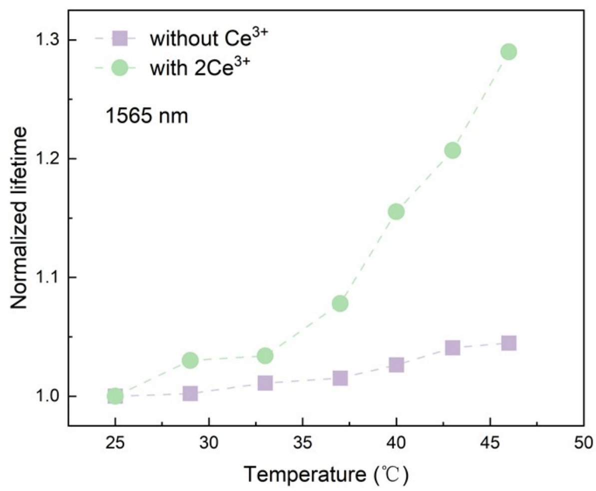

Fig. S4. Temperature-dependent luminescence decays of $NaYF_4$:$5Er^{3+}$/$2Ce^{3+}$@$NaYbF_4$@$NaYF_4$:$40Nd^{3+}$/$20Yb^{3+}$ and $NaYF_4$:$5Er^{3+}$@$NaYbF_4$ @$NaYF_4$:$40Nd^{3+}$/$20Yb^{3+}$ nanoparticles dispersed in deionized water. Excitation at 808 nm, emission at 1565 nm.

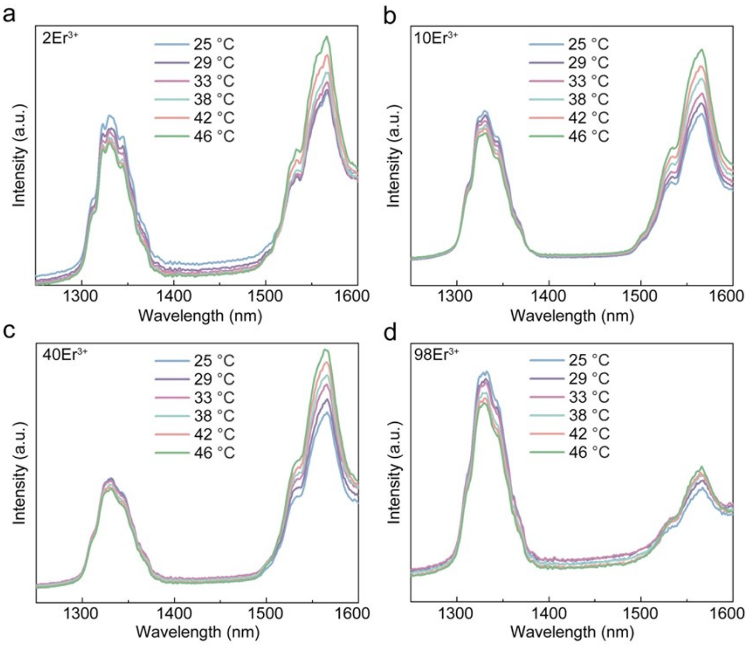

Fig. S5. Temperature-dependent emission spectra of the $NaYF_4$:xEr^{3+}/2Ce^{3+}@$NaYbF_4$@$NaYF_4$:40Nd^{3+}/20Yb^{3+} nanocrystals: (a) 2Er^{3+}, (b) 10Er^{3+}, (c) 40Er^{3+} and (d) 98Er^{3+}.

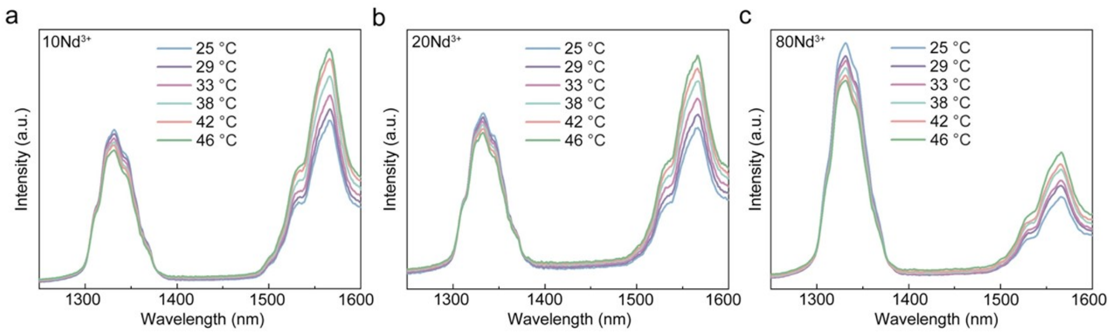

Fig. S6. Temperature-dependent emission spectra of the $NaYF_4$:5Er^{3+}/2Ce^{3+}@$NaYbF_4$@$NaYF_4$:yNd^{3+}/20Yb^{3+} nanocrystals: (a) 10Nd^{3+}, (b) 20Nd^{3+} and (c) 80Nd^{3+}.

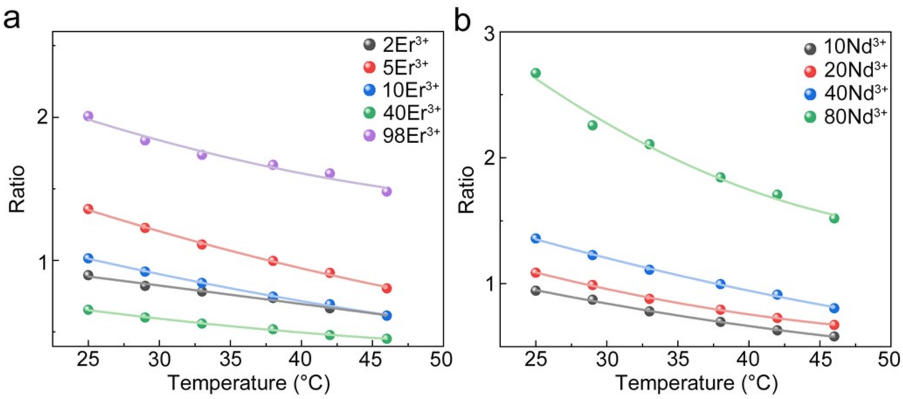

Fig. S7. The change in *R* with temperature for nanoparticles with different (a) Er^{3+} doping concentrations and (b) Nd^{3+} doping concentrations.

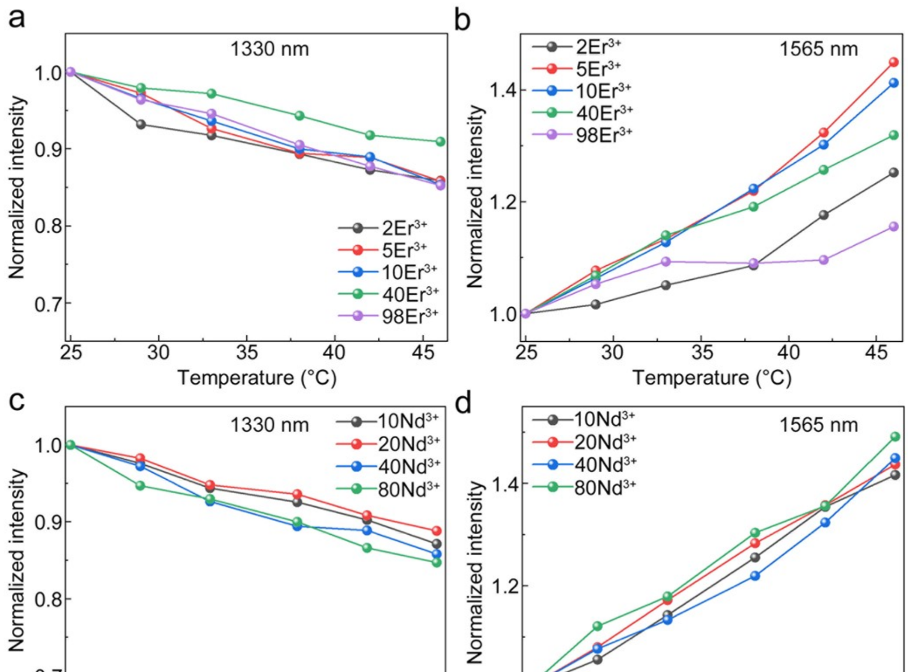

Fig. S8. Normalized 1330 emission intensity against the temperature with varying (a) Er^{3+} doping concentrations, and (c) Nd^{3+} doping concentrations. Normalized 1565 nm emission intensity against the temperature with varying (b) Er^{3+} doping concentrations, and (d) Nd^{3+} doping concentrations.

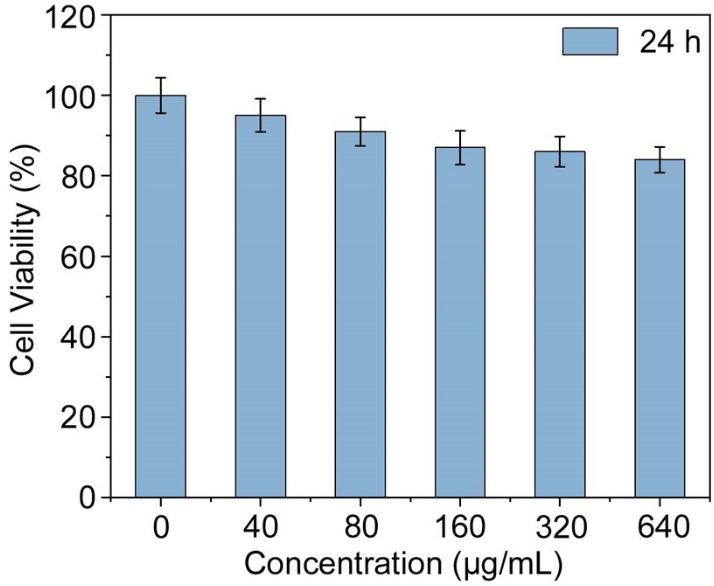

Fig. S9. 4T1 cells viability after co-incubation with NPs of different concentrations for 24 h.

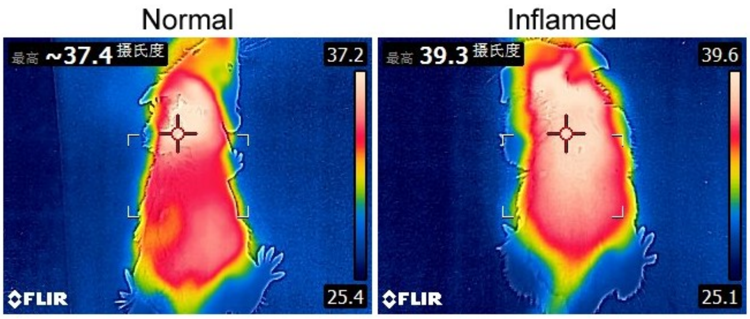

Fig. S10. Skin temperature of the (a) normal and (b) inflamed mice captured by a thermal camera.

Table S1. The fitting parameters of calibration curve for $NaYF_4$:xEr^{3+}/2Ce^{3+}@$NaYbF_4$@$NaYF_4$:40Nd^{3+}/20Yb^{3+} nanoparticles with different Er^{3+}.

Doping ratio	*a*	*b*	*c*	R^2
2%	1.19228	-0.01184	-1.46308×10^{-5}	0.98897
5%	2.28908	-0.04391	2.57113×10^{-4}	0.99781
10%	1.68023	-0.03113	1.75002×10^{-4}	0.99698
40%	1.06325	-0.02018	1.49829×10^{-4}	0.9965
98%	3.00147	-0.05051	3.91609×10^{-4}	0.97468

Table S2. The fitting parameters of calibration curve for $NaYF_4$:5Er^{3+}/2Ce^{3+}@$NaYbF_4$@$NaYF_4$:yNd^{3+}/20Yb^{3+} nanoparticles with different Nd^{3+}.

Doping ratio	*a*	*b*	*c*	R^2
10%	1.65079	-0.03376	2.26922×10^{-4}	0.99839
20%	2.04657	-0.04842	4.03760×10^{-4}	0.99881
40%	2.28908	-0.04391	2.57113×10^{-4}	0.99781
80%	5.34230	-0.13729	0.00119	0.99606